Cancer Chemother Pharmacol (2000) 46: 156–166

ORIGINAL ARTICLE

Ellyn M. Sharkey · Hugh B. O'Neill
Malcolm J. Kavarana · Haibo Wang
Donald J. Creighton · Dorothy L. Sentz
Julie L. Eiseman

Pharmacokinetics and antitumor properties in tumor-bearing mice of an enediol analogue inhibitor of glyoxalase I

Received: 1 November 1999 / Accepted: 20 March 2000

Abstract *Purpose*: The enediol analogue *S*-(*N*-*p*-chlorophenyl-*N*-hydroxycarbamoyl)glutathione (CHG) is a powerful, mechanism-based, competitive inhibitor of the methylglyoxal-detoxifying enzyme glyoxalase I. The [glycyl,glutamyl]diethyl ester prodrug form of this compound ($CHG(Et)_2$) inhibits the growth of different tumor cell lines in vitro, apparently by inducing elevated levels of intracellular methylglyoxal. The purpose of this study was to evaluate the pharmacokinetic properties of $CHG(Et)_2$ in plasma esterase-deficient C57BL/6 (Es-1^e) mice after intravenous (i.v.) or intraperitoneal (i.p.) administration of bolus doses of $CHG(Et)_2$. In addition, the in vivo antitumor properties of $CHG(Et)_2$ were evaluated against murine B16 melanoma in these mice, and against androgen-independent human prostate PC3 tumor and human colon HT-29 adenocarcinoma in plasma esterase-deficient nude mice. *Methods*: Pharmacokinetics were evaluated after either i.v. or i.p. administration of $CHG(Et)_2$ at the maximally tolerated dose of 120 mg/kg to both tumor-free male and female mice and male and female mice bearing subcutaneous B16 tumors. Tissue concentrations of $CHG(Et)_2$, CHG and the [glycyl]monoethyl ester CHG(Et) were measured as a function of time by reverse-phase C_{18} high-performance liquid chromatography of deproteinized tissue samples. The efficacy of $CHG(Et)_2$ in tumor-bearing mice was evaluated after i.v. bolus administration of $CHG(Et)_2$ at 80 or 120 mg/kg for 5 days each week for 2 weeks, or after 14 days continuous infusion of $CHG(Et)_2$ using Alzet mini-osmotic pumps. Hydroxypropyl-β-cyclodextrin was used as a vehicle in the efficacy studies. *Results*: Intravenous administration of $CHG(Et)_2$ resulted in the rapid appearance of $CHG(Et)_2$ in the plasma of tumor-bearing mice with a peak value of 40–60 μM, followed by a first-order decrease with a half-life of about 10 min. There was a corresponding increase in the concentration of inhibitory CHG in the B16 tumors, with a maximum concentration in the range 30–60 μM occurring at 15 min, followed by a decrease to a plateau value of about 6 μM after 120 min. Neither $CHG(Et)_2$ nor its hydrolysis products were detectable in plasma, after i.p. administration of $CHG(Et)_2$ to tumor-free female mice. From the efficacy studies, dosing schedules were identified that resulted in antitumor effects comparable to those observed with the standard antitumor agents Adriamycin (with B16 tumors), cisplatin (with PC3 tumors), and vincristine (with HT-29 tumors). *Conclusion:* This is the first demonstration that a mechanism-based competitive inhibitor of glyoxalase I effectively inhibits the growth of solid tumors in mice when delivered as the diethyl ester prodrug.

Key words *S*-(*N*-*p*-chlorophenyl-*N*-hydroxycarbamoyl) glutathione · Glyoxalase I inhibitor · Pharmacokinetics · In vivo efficacy

Supported by grant CA 59612, awarded by the National Cancer Institute

E. M. Sharkey · H. B. O'Neill
M. J. Kavarana · H. Wang · D. J. Creighton
Department of Chemistry and Biochemistry,
University of Maryland, Baltimore County,
Baltimore, MD 21250, USA

D. L. Sentz · J. L. Eiseman
Division of Developmental Therapeutics,
Greenebaum Cancer Center and Department of Pathology,
University of Maryland,
Baltimore, MD 21201, USA

Introduction

Competitive inhibitors of glyoxalase I have long been proposed as possible anticancer agents because of their potential ability to induce elevated levels of cytotoxic methylglyoxal in tumor cells [22]. In 1992, Lo and Thornalley obtained experimental support for this hypothesis with the demonstration that the glyoxalase I inhibitor, *S*-*p*-bromobenzylglutathione, is efficiently delivered into human leukemia HL60 cells as the diethyl ester prodrug and inhibits cell growth [11]. Work carried out in the same laboratory subsequently showed that the

dicyclopentyl ester prodrug is cytostatic to several different human tumors in vitro [20], and a murine adenocarcinoma in vivo [19]. Glyoxalase I inhibitors are potentially selective tumoricidal agents, as extracellular methylglyoxal is known to inhibit preferentially the growth of rapidly dividing tumor cells as compared to quiescent normal cells in tissue culture [2, 4, 14, 15]. Selective toxicity might be due to inhibition of DNA synthesis [15, 24]. Indeed, methylglyoxal is known to form covalent adducts with both proteins and nucleic acids [13].

We recently evaluated the in vitro antitumor properties of three mechanism-based competitive inhibitors of glyoxalase I as the diethyl ester prodrugs, e.g. the [glycyl,glutamyl]diethyl ester prodrug form of *S*-(*N*-*p*-chlorophenyl-*N*-hydroxycarbamoyl)glutathione (CHG) ($CHG(Et)_2$; Fig. 1) [10]. CHG is one of the strongest competitive inhibitors of human glyoxalase I yet reported (K_i 40 n*M*). $CHG(Et)_2$ inhibits the growth of L1210 murine leukemia (GI_{50} 7 μM) and the solid murine tumor B16 melanotic melanoma (GI_{50} 15 μM) in vitro. Growth inhibition is accompanied by rapid esterase-catalyzed conversion of $CHG(Et)_2$ to the inhibitory diacid CHG inside the cells. That growth inhibition reflects inhibition of glyoxalase I is consistent with the observation that preincubation of L1210 cells with $CHG(Et)_2$ increases the sensitivity of the cells to inhibition by extracellular methylglyoxal [10]. Moreover, L1210 cells are more sensitive than murine splenic lymphocytes to the inhibitory effects of $CHG(Et)_2$. This could reflect the greater intrinsic sensitivity of rapidly dividing cells to methylglyoxal. Also, selectivity could arise from the ten-fold lower activity of glyoxalase II in L1210 cells as compared to splenic lymphocytes [10]. Because CHG is slowly hydrolyzed by GlxII, CHG might be more stable in L1210 cells and, therefore, more toxic to these cells. This mechanism of selective toxicity might apply generally, as many different types of cultured and excised tumors contain abnormally low levels of glyoxalase II activity, including the three tumor types examined in the current study [3, 6, 8].

We describe here the pharmacokinetics and antitumor properties of $CHG(Et)_2$ in plasma esterase-deficient C57BL/6 (Es-1^e) mice bearing murine B16 melanoma, and in esterase-deficient athymic nude mice bearing androgen-independent human prostate PC3 or human colon HT-29 xenografts. The importance of the plasma esterase-deficient mice used in this study is that they model the low esterase activity in human plasma [10]. This is the first systematic preclinical evaluation of the chemotherapeutic potential of a mechanism-based competitive inhibitor of glyoxalase I.

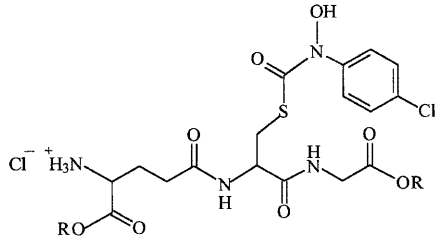

S-(N-p-chlorophenyl-N-hydroxycarbamoyl)glutathione (R = H)

(CHG; NSC 693567)

S-(N-p-chlorophenyl-N-hydroxycarbamoyl)glutathione diethyl ester (R = C_2H_5)

($CHG(Et)_2$; NSC 693569)

S-(N-p-chlorophenyl-N-hydroxycarbamoyl)glutathione dicyclopentyl ester

(R = cyclo C_5H_9)

($CHG(cyclopentyl)_2$)

Fig. 1 Structures of the glyoxalase I inhibitor CHG and its diethyl ester $CHG(Et)_2$ and dicyclopentyl ester $CHG(cyclopentyl)_2$ prodrugs. CHG is a stable analogue of the tightly bound enediolate intermediate that forms along the reaction coordinate glyoxalase I

Materials and methods

Reagents

The glyoxalase I inhibitor CHG was synthesized via an acyl interchange reaction between glutathione and *N*-*p*-chlorophenyl-*N*-hydroxycarbamate *p*-chlorophenyl ester, as previously described by this laboratory [12]. This procedure was scaled up to produce gram quantities of CHG as follows. A solution of freshly synthesized and crystallized *N*-*p*-chlorophenyl-*N*-hydroxycarbamate *p*-chlorophenyl ester (4.6 g, 15.5 mmol) was prepared in 350 ml absolute ethanol. To this solution was added over a period of approximately 30 min with stirring a freshly prepared solution of glutathione (29 g, 84.6 mmol) in degassed nitrogen-saturated water at pH 9.5. The reaction mixture was placed under an atmosphere of nitrogen and stirred at room temperature until little acylating agent remained (about 24 h) as judged by silica gel TLC (*n*-propanol/acetic acid/water, 10:1:5 v/v/v). The acylating reagent and the product had R_f values of 0.89 (UV) and 0.61 (UV, ninhydrin), respectively.

The reaction mixture was adjusted to a pH meter reading of 3.5 with 6 *N* HCl and the solvent removed in vacuo. The white residue was suspended in 200 ml water and stirred at room temperature overnight. The solid was removed by filtration, suspended in 250 ml water and stirred for about 6 h. The white precipitate was again collected by filtration and thoroughly dried under vacuum. In order to remove unreacted acylating reagent and *p*-chlorophenol, the precipitate was suspended in 300 ml diethyl ether and stirred overnight. This washing procedure was repeated two more times (stir times of about 3 h) in order to remove the last traces of acylating reagent and *p*-chlorophenol as judged by silica gel TLC (yield 60%; analytical data identical to literature values [12]). The corresponding diethyl ester $CHG(Et)_2$ was prepared by incubation of CHG in 6.2 *N* ethanolic HCl at room temperature until diesterification was >95% complete (about 8 h). The progress of the reaction was monitored by reverse phase C_{18} column chromatography (Waters μBondapak C_{18}, 7.8 × 300 mm), using 0.25% acetic acid and 40% methanol in water as an eluting solvent (2 ml/min). The approximate retention times were as follows: $CHG(Et)_2$ 76 min, CHG 27 min, CHG[glycyl](Et) 62 min. The dicyclopentyl diester $CHG(cyclopentyl)_2$ was similarly prepared by incubating CHG in cyclopentanol/HCl.

The metabolites *S*-(*N*-*p*-chlorophenyl-*N*-hydroxycarbamoyl) cysteinylglycine and *S*-(*N*-*p*-chlorophenyl-*N*-hydroxycarbamoyl) cysteine were prepared by partial hydrolysis of CHG using the peptidases present in mouse kidney homogenate. To 5 ml of a

60 m*M* solution of CHG at pH 7 was added 1.5 ml kidney homogenate at room temperature. The kidney homogenate was obtained by combining one volume of kidney with two volumes of ice water and homogenizing the mixture with a Tissue Tearor at maximum speed (25,000–30,000 rpm) on ice for 30 s. The progress of the hydrolysis reaction was followed by removing aliquots from the incubation mixture as a function of time and fractionating the aliquots on a reverse-phase HPLC (Waters μBondapak C_{18}, 7.8 × 300 mm), using methanol/water (2:3) containing 0.25% acetic acid as a running solvent (2 ml/min). The approximate retention times were 27 min for CHG, 22 min for *S*-(*N*-*p*-chlorophenyl-*N*-hydroxycarbamoyl)cysteine, and 19 min for *S*-(*N*-*p*-chlorophenyl-*N*-hydroxycarbamoyl)cysteinylglycine.

When the concentration of CHG had decreased to 25% of its original value, protein was precipitated from the incubation mixture by the addition of a threefold volume excess of 95% ethanol in water containing 0.25% acetic acid. The protein precipitate was removed by centrifugation and the metabolites isolated from the supernatant by reverse-phase HPLC as described above (yields: *S*-(*N*-*p*-chlorophenyl-*N*-hydroxycarbamoyl)cysteinylglycine, 12%; *S*-(*N*-*p*-chlorophenyl-*N*-hydroxycarbamoyl)cysteine, 71%). The chemical identities of the two metabolites were confirmed by ^{1}H 300 MHz NMR and fast-atom bombardment mass spectrometry.

Dosing solutions were prepared by dissolution of $CHG(Et)_2$ in vehicle solutions composed of either a mixture of cremophor/ethanol/50 m*M* sodium phosphate buffer (pH 7; 1:1:6 v/v/v) or 20% hydroxypropyl-β-cyclodextrin (HP-β-CD; Sigma) in water. Dosing solutions were sterilized by filtration through a sterile 0.45-μm filter.

Mice

Adult plasma esterase-deficient male and female C57BL/6 (Es-1^e) mice and adult plasma esterase-deficient male and female athymic nude C57BL/6 (Es-1^e) nu/nu mice were purchased from Jackson Laboratories (Bar Harbor, Me.). The pathogen-free mice were allowed to acclimate to the University of Maryland, Baltimore, Animal Facility for at least 1 week before studies were initiated. The mice were handled in accordance with the Guide for the Care and Use of Laboratory Animals (National Research Council, 1996) in animal rooms on automatic 12-h light/dark cycles with at least 12 air changes per hour, and temperatures maintained at 72 ± 2 °F. Mice were housed in autoclaved microisolator caging and fed Teklad autoclavable rodent chow and autoclaved water ad libitum except in the pharmacokinetic studies where, on the evening prior to dosing, all food was removed and withheld until 4 h after dosing. Sentinel mice were maintained in cages containing one-fifth dirty bedding obtained from the study mice. The sentinel mice remained free of murine-specific pathogens as determined by murine antibody profile (MAP) testing (Litton Bionetics, Charleston, S.C.) conducted monthly throughout the study period. All studies performed were approved by the Animal Care and Use Committee at the University of Maryland, Baltimore, Maryland, and the University of Maryland, Baltimore County, Baltimore, Maryland.

Pharmacokinetic sampling

Either $CHG(Et)_2$ or vehicle was administered to the mice intravenously (i.v.) by a lateral tail vein as a 30-s bolus and generally three mice were euthanized with CO_2 at the following time-points after dosing: 5, 10, 15, 30, 45, 60, 90, 120, 180, 240, 360, 420, 960, and 1440 min. Blood samples were obtained by cardiac puncture using heparinized syringes and needles, transferred to Eppendorf microfuge tubes and stored on ice until centrifugation at 13,000 rpm for 4 min to separate plasma and red blood cells. Tissues including liver, kidney, spleen, testis, brain and tumors were excised, placed on ice, weighed and snap-frozen in liquid nitrogen. Urine and feces were collected over ice from the mice euthanized at 960 and 1440 min. Plasma, red cells, urine and tissue samples were stored at −70 °C until analysis.

Analysis of $CHG(Et)_2$ and metabolites

In brief, sample preparation was carried out as follows. Samples of plasma (300 μl) were deproteinized using 1 ml 95% ethanol in water containing 0.25% acetic acid. Following centrifugation, the supernatant was removed and the pellet washed once with 200 μl denaturing solvent. The wash and supernatant fractions were pooled, brought to dryness under a stream of dry air, and the residue analyzed by HPLC. Samples of red blood cells (200 μl) were lysed with 200 μl 2.5% aqueous acetic acid then deproteinized with 100 μl 10% sulfosalicylic acid in water. After centrifugation, the supernatant was removed and brought to dryness under a stream of dry air. The residue was dissolved in 200 μl running solvent and analyzed by HPLC. Whole frozen melanoma tumor, kidney, liver, spleen, testis or brain was combined with two volumes of water and homogenized with a Tissue Tearor at maximum speed (25,000–30,000 rpm) on ice for 30 s. The tissue homogenates (50–500 μl) were then deproteinized using three volumes of 95% ethanol in water, containing 0.25% acetic acid. After centrifugation, the pellets were washed once with denaturing solvent and the wash and supernatant fractions combined. This mixture was brought to dryness under a stream of dry air. The residue was dissolved in 200 μl running solvent and analyzed by reverse-phase HPLC with UV detection.

HPLC was carried out using a Shimadzu liquid chromatography system composed of dual LC-6A pumps, SIL-10A autoinjector, and SCL-10A system controller. Tissue extracts were fractionated by isocratic elution from a Waters μBondapak C_{18} column (7.8 × 300 mm). Column effluents were monitored at 260 nm using a Shimadzu SPD-6AV UV-VIS spectrophotometric detector. The output signal was processed with a Shimadzu CR601 Chromatopac, which gives the integrated area under the peaks. Good baseline separations were generally achieved for $CHG(Et)_2$ and the major metabolites CHG(Et) and CHG using methanol/water (2:3) containing 0.25% acetic acid as a running solvent (see for example Fig. 2). In some cases, the ratio of methanol to water was changed slightly in order to improve the separations.

The concentrations of $CHG(Et)_2$, CHG(Et), and CHG were determined by comparison of the integrated intensities of the corresponding peaks with the appropriate standard curves. The standard curves were generated by extraction of known amounts of these materials from the same tissues. For all three compounds, there were no endogenous interfering peaks and the inter- and intraday assay covariances were 10%. Standard curves were prepared in triplicate and were linear between 0.02 nmol and 50 nmol. The lower limit of quantitation, defined as a signal-to-noise ratio of 10:1, was 0.02 nmol. Yields of $CHG(Et)_2$, CHG(Et) and CHG from plasma were greater than 90%. Yields of CHG(Et) and CHG from red blood cells were 25–30%. Yields of CHG(Et) and CHG from the other tissues were approximately 65%.

The binding of $CHG(Et)_2$ to plasma proteins was determined by first placing solutions of $CHG(Et)_2$ (30–130 μM) in mouse plasma or in running solvent (methanol/water 2:3, with 0.25% acetic acid) into Amicon Centrifree ultrafiltration devices (Amicon Division of W.R. Grace, Beverly, Mass.). Filtrates were obtained by centrifugation at 2000 *g* for 20 min. Concentrations of $CHG(Et)_2$ in the filtrates were determined by HPLC as described above. The percentage bound was calculated from the difference in peak areas for $CHG(Et)_2$ in filtered running solvent versus that in filtered plasma.

Analysis of pharmacokinetic data

The time-dependent changes in the plasma and tissue concentrations of $CHG(Et)_2$ and its metabolites were analyzed by both noncompartmental and compartmental methods. Areas under the curves from zero to infinity (AUC) and terminal rate constants (k_{el}) were obtained by noncompartmental analysis using the program LAGRAN, which uses the LaGrange function [17]. The clearance rate (CL) was calculated from the definition CL = dose/AUC, and the steady-state volume of distribution (Vd_{ss}) was calculated from

the formula $Vd_{ss} = dose \times AUMC/AUC^2$, where AUMC is the area under the moment curve from zero to infinity. Compartmental analysis was performed using the program ADAPT II [5] with generalized least squares estimation and a five-compartment open linear model with first-order absorption into compartment 1 from compartment 0.

Analysis of enzyme activities and competitive inhibition constants

The activities of glyoxalases I and II in mouse tissues were determined as follows. To a frozen tissue sample on ice were added 12 volumes of an ice-cold solution of sodium phosphate buffer (50 m*M*, pH 7), containing 0.1 m*M* phenylmethanesulfonyl fluoride and 0.5% ethanol. The mixture was homogenized on ice with a Tissue Tearor at maximum speed and centrifuged at 20,000 *g* to remove cell debris. The supernatant was reserved for enzyme assays. For glyoxalase I activity, the V_m and K_m values were obtained from the variation of the initial rate of formation of *S*-D-lactoylglutathione ($\Delta\varepsilon$ 2860 $cm^{-1}M^{-1}$) as a function of glutathione-methylglyoxal thiohemiacetal concentration in the range 0.02–0.4 m*M*. The concentration of free glutathione was maintained at 0.1 m*M*, on the basis of a dissociation constant for the thiohemiacetal of 2.2 m*M*. For glyoxalase II activity, the V_m and K_m values were obtained from the variation of the initial rate of loss of *S*-D-lactoylglutathione ($\Delta\varepsilon$ 3300 $cm^{-1}M^{-1}$) as a function of *S*-D-lactoylglutathione concentration in the range 0.03–0.5 m*M*. Kinetic constants were obtained from hyperbolic fits of the initial rate data to the Michaelis-Menten equation. Protein concentrations were determined with a protein assay kit (Bio-Rad), using bovine serum albumin as a reference standard.

Inhibition constants were obtained from the variation of the apparent K_m of glyoxalase I in the presence of different inhibitor concentrations, according to the equation for competitive inhibition [12].

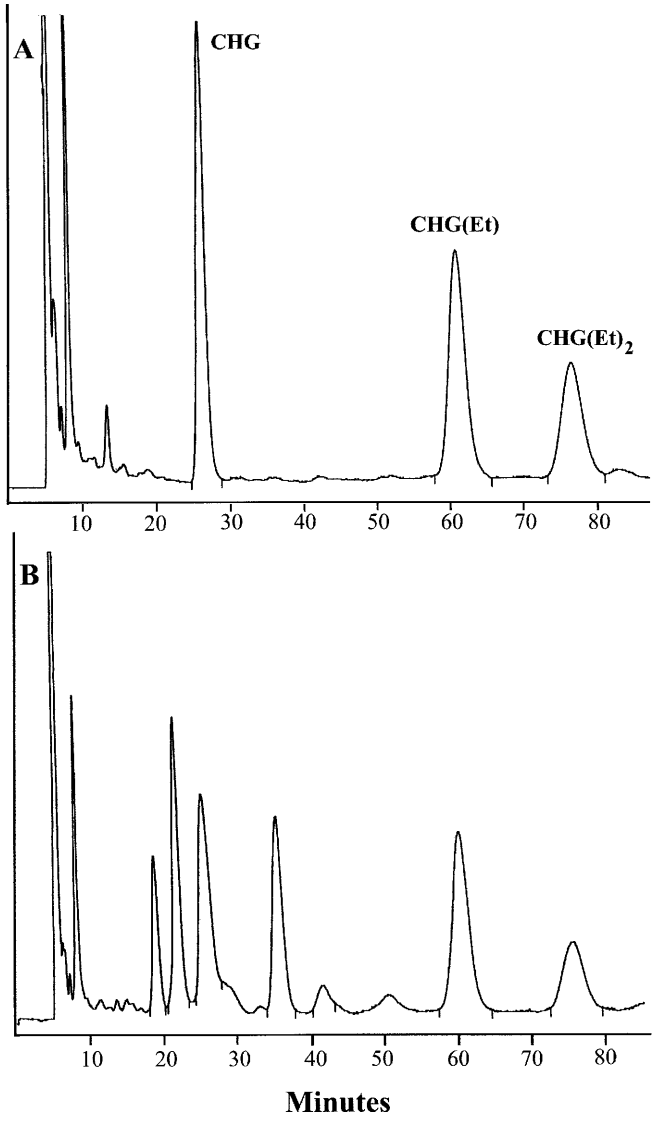

Fig. 2A,B HPLC elution profiles of (**A**) control mouse plasma spiked with authentic CHG (1.7 nmol), CHG(Et) (1.7 nmol) and $CHG(Et)_2$ (1.4 nmol), and (**B**) mouse plasma (25 μl) obtained from a C57/BL6 (Es-1^e) mouse 5 min after a single bolus i.v. administration at 120 mg/kg $CHG(Et)_2$. The peaks at 19 and 22 min comigrate with authentic samples of S-(N-p-chlorophenyl-N-hydroxycarbamoyl)cysteinylglycine and S-(N-p-chlorophenyl-N-hydroxy-carbamoyl)cysteine, respectively

Efficacy studies

B16 melanotic melanoma was obtained from the NCI tumor repository (Frederick, Md.), and HT-29 human colon adenocarcinoma and human prostate PC3 cells were obtained from the ATCC (Rockville, Md.). Tumors were expanded in passage mice and fragments of tumors (25 mg) were stored frozen in liquid nitrogen until needed. The tumor fragments were implanted subcutaneously into the right flank of passage mice. When the tumors reached about 500 mm^3 by caliper measurements, the mice were euthanized, the tumors were removed aseptically and fragments of about 25 mg were implanted s.c. into the right flank of the study mice on day 0. After the tumors were established, the mice were stratified into groups of ten such that the mean and median tumor volumes of each treatment group were not different from any other treatment group. The drugs were administered by i.v. bolus injection by a lateral tail vein, or by constant i.v. infusion using 14-day Alzet miniosmotic pumps and catheters into the external jugular vein. Dosing schedules are given in the figure legends. Tumor dimensions, measured using a digital caliper, and body weights and clinical observations were recorded twice weekly. Tumor volumes were calculated using the formula $T_{vol} = L \times W^2/2$, where L is the longest diameter of the tumor and W is the shortest diameter perpendicular to L. Implantation of the 14-day Alzet pumps followed the directions supplied by the manufacturer. The pumps were calibrated to deliver a 0.6 *M* solution of $CHG(Et)_2$ in 20% HP-β-CD i.v. at a rate of 0.5 μl/h.

Statistical evaluation of the efficacy studies

Differences in tumor volumes, body weights and tissue weights among test and control groups were analyzed by parametric and nonparametric methods. Mean data were compared using one-way analysis of variance (ANOVA), followed by pair-wise comparisons using Dunnett's test. Median data were compared by nonparametric analysis using the Kruskal-Wallis test, and pair-wise comparisons were done using the Mann-Whitney test. Significance was set at $P \leq 0.05$. Calculations were done with the Minitab statistical software package (Minitab, State College, Pa.).

Results

Glyoxalase activities in mouse tissues

In preparation for the pharmacokinetic and efficacy studies, the activities of the two glyoxalase enzymes were first determined in different tissues of C57BL/6 (Es-1^e)

mice implanted with B16 tumors (Table 1). The V_m activities of both enzymes in melanoma extract were 2- to 12-fold lower than the activities in the normal tissues.

Range-finding study

Initial efforts were directed at identifying the maximum tolerated dose of $CHG(Et)_2$ in C57BL/6 (Es-1^e) mice. In the initial study, one male and one female mouse were treated at doses of 120 mg/kg i.v. as both rapid bolus (over less than 30 s) and a slow bolus (over 60 s). The mice that received the slow bolus survived and appeared normal at 24 h after dosing. The mice that received the rapid bolus convulsed and died. Because the mice receiving the slow bolus survived, groups of five male and five female mice were used for each dosing group and drug was delivered as a slow bolus at doses of 120, 80 and 53 mg/kg. The mice receiving the highest dose lost righting reflex for approximately 2–5 min after dosing and remained sedated for approximately 4 h. Within 48 h of dosing there was localized necrosis at the injection site. This effect was dose-dependent, as the effect was less severe in mice receiving lower doses and was not observed in mice receiving vehicle only. When the animals were euthanized 14 days after administration of the highest dose, their body weights were about 10% less than the body weights of the groups receiving lower doses, the vehicle groups and the untreated controls. The body weights of the mice receiving 120 mg/kg $CHG(Et)_2$ via intraperitoneal (i.p.) injection were not significantly different from those of the vehicle group. Necropsy of all test groups showed that the weights of spleen, kidney and testicles were not significantly different from those of the vehicle-treated group. Thus, 120 mg/kg was selected as the highest dose to be used in the pharmacokinetic study.

Pharmacokinetics

Pharmacokinetic data were acquired for both B16 tumor-bearing and nontumor-bearing male and female C57BL/6 (Es-1^e) mice after i.v. bolus injection of $CHG(Et)_2$ at 120 mg/kg. The magnitudes of the kinetic constants derived from non-compartmental analysis of the kinetic data were similar for the different groups (Tables 2 and 3). Plasma pharmacokinetics showed that $CHG(Et)_2$ was rapidly cleared from plasma, with half-lives in the range of 5 to 13 min for all groups. The loss of $CHG(Et)_2$ was accompanied by the rapid appearance and subsequent loss of both CHG(Et) and CHG (see for example Fig. 3A). However, the loss of $CHG(Et)_2$ is unlikely to have been due simply to hydrolysis of the diester. This assertion is based on the results of fitting the data to a five-compartment open linear model with first-order absorption. The rapid loss of $CHG(Et)_2$ from plasma appears to have been due primarily to the rapid and extensive extravascular distribution of $CHG(Et)_2$ into the tissues of the mouse, as the hydrolysis of $CHG(Et)_2$ was a relatively slow process (k_{12} 0.017–0.006 min^{-1}; $T_{1/2}$ 41–116 min) in comparison to the rate of non-hydrolytic loss of $CHG(Et)_2$ (k_{10} 0.23–1.1 min^{-1}; $T_{1/2}$ 0.63–3.0 min) (Table 4, Fig. 4).

No $CHG(Et)_2$ was found in the urine or feces of the mice from the different groups. Moreover, noncompartmental analysis of the tissue distribution of these compounds showed that the loss of $CHG(Et)_2$ from plasma was accompanied by extensive and rapid appearance of CHG(Et) and CHG within the different tissues of the mouse (Tables 2 and 3). Importantly, the concentration of CHG in subcutaneous melanoma increased to a maximum concentration in the range 25–46 μM after 15 min, followed by a decrease to a plateau value of about 7 μM after 120 min (Fig. 3A). This concentration was maintained over approximately 6 h. Red blood cells also acquired high concentrations of both CHG and CHG(Et), which were maintained over several hours (Fig. 3B).

The HPLC profile of mouse plasma showed two additional peaks that comigrated with authentic samples of *S*-(*N*-*p*-chlorophenyl-*N*-hydroxycarbamoyl)cysteinylglycine (19 min) and *S*-(*N*-*p*-chlorophenyl-*N*-hydroxycarbamoyl)cysteine (22 min) (Fig. 2). The presence of these compounds in plasma probably arose from the action of kidney peptidases on CHG [23], and probably made an important contribution to the magnitude of k_{30} (Table 4). An additional unidentified peak was found at 35 min with a half-life of approximately 5 min.

Neither $CHG(Et)_2$ nor its hydrolysis products could be detected in the plasma of mice after i.p. injection of $CHG(Et)_2$ at 120 mg/kg, indicative of rapid degradation

Table 1 Glyoxalase activities in the tissues of plasma esterase-deficient C57BL/6 (Es-1^e) mice bearing B16 melanotic melanoma

Tissue	Glyoxalase I[a]			Glyoxalase II[b]		
	Specific activity (U/mg)	K_m (mM)	n[c]	Specific activity (U/mg)	K_m (mM)	n[c]
Liver	4.48 ± 0.62	0.09 ± 0.01	3	0.66 ± 0.85	0.24 ± 0.03	3
Kidney	1.06 ± 0.40	0.07 ± 0.01	3	0.60 ± 0.67	0.16 ± 0.01	3
Brain	1.15 ± 0.35	0.07 ± 0.01	3	0.25 ± 0.23	0.15 ± 0.02	3
Spleen	1.13 ± 0.13	0.09 ± 0.01	3	0.13 ± 0.13	0.23 ± 0.02	3
Melanoma	0.37 ± 0.16	0.07 ± 0.01	4	0.07 ± 0.18	0.19 ± 0.06	4

[a] Conditions: potassium phosphate buffer, 50 mM, pH 7, 25 °C
[b] Conditions: TRIS buffer, 20 mM, pH 7.4, 25 °C
[c] Number of animals

Table 2 Non-compartmental analysis of the pharmacokinetic data for female C57BL/6 (Es-1[e]) mice after i.v. administration of $CHG(Et)_2$ at 120 mg/kg (*ND* not determined)

Tissue	Metabolite	B16-bearing					Non-tumor-bearing				
		C_{max} (μM)	T_{max} (min)	$T_{1/2}$ (min)	AUC ($\mu M \cdot$ min)	CL (ml $\cdot$ min^{-1} $\cdot$ kg^{-1})	C_{max} (μM)	T_{max} (min)	$T_{1/2}$ (min)	AUC ($\mu M \cdot$ min)	CL (ml $\cdot$ min^{-1} $\cdot$ kg^{-1})
Plasma	$CHG(Et)_2$	27[a]	5	5	220	960	23[a]	5	13	310	680
	CHG(Et)	92	45	97	16,500	13	100	25	90	15,000	15
	CHG	23	5	25	610	390	15	10	9	355	660
RBCs	CHG(Et)	294	30	294	125,000	2	580[a]	2	277	120,000	2
	CHG	91	15	788	33,600	6	27	15	231	5,000	42
Liver	CHG(Et)	ND	ND	ND	ND	ND	21	15–60	72	2,300	93
	CHG	79	5	173	2,070	102	73	10	126	5,500	38
Brain	CHG[b]	2	10	108	58	3,600	3	45	48	163	1,300
Spleen	CHG[c]	1500	5	98	120,000	2	1,800	10	95	180,000	1
Sk. muscle	CHG(Et)	–	–	–	–	–	34	10	145	3,251	65
	CHG	–	–	–	–	–	33	25	143	8,386	25
Heart	CHG(Et)	–	–	–	–	–	65	10	296	11,750	18
	CHG	–	–	–	–	–	137	15	80	10,150	21
Lung	CHG(Et)	–	–	–	–	–	89	10	135	18,054	12
	CHG	–	–	–	–	–	149	10	75	10,767	20
B16	CHG[d]	46	15	228	3,600	59	–	–	–	–	–

[a] Concentration at earliest time point; no clear peak detected
[b] Traces of $CHG(Et)_2$ detected below the limit of quantitation
[c] CHG(Et) not detected
[d] CHG(Et) detected, but not quantitated

Table 3 Non-compartmental analysis of the pharmacokinetic data for male C57BL/6 (Es-1[e]) mice after i.v. administration of $CHG(Et)_2$ at 120 mg/kg (*ND* not determined)

Tissue	Metabolite	B16-bearing					Non-tumor-bearing				
		C_{max} (μM)	T_{max} (min)	$T_{1/2}$ (min)	AUC ($\mu M \cdot$ min)	CL (ml $\cdot$ min^{-1} $\cdot$ kg^{-1})	C_{max} (μM)	T_{max} (min)	$T_{1/2}$ (min)	AUC ($\mu M \cdot$ min)	CL (ml $\cdot$ min^{-1} $\cdot$ kg^{-1})
Plasma	$CHG(Et)_2$	20[a]	5	11	620	340	12[a]	5	7	220	970
	CHG(Et)	78	30	86	14,000	16	86	25	77	10,000	22
	CHG	39[a]	5	10	780	300	21	5	57	680	350
RBCs	CHG(Et)	2,400[a]	5	139	149,000	1	900[a]	2	215	178,000	1
	CHG	410[a]	5	96	12,300	17	89[a]	2	50	4,100	51
Liver	CHG(Et)	61	15	92	4,500	47	26	25	53	1,600	136
	CHG	1,060[a]	5	98	17,000	12	140[a]	2	83	9,500	22
Brain	CHG[b]	ND	ND	ND	ND	ND	ND	ND	ND	ND	ND
Spleen	CHG[c]	1,600[a]	5	83	177,000	1	1,390	10	42	103,000	2
Sk. muscle	CHG(Et)	–	–	–	–	–	42	10	133	8,141	26
	CHG	–	–	–	–	–	48	5	240	8,917	24
Heart	CHG(Et)	–	–	–	–	–	59	20	75	5,570	38
	CHG	–	–	–	–	–	148	10	86	9,368	22
Lung	CHG(Et)	–	–	–	–	–	145	45	144	20,131	10
	CHG	–	–	–	–	–	141	5	178	14,608	14
B16	CHG(Et)	22	30–60	63	2,200	97	–	–	–	–	–
	CHG	25	15	116	2,900	50	–	–	–	–	–

[a] Concentration at earliest time point; no clear peak detected
[b] Traces of $CHG(Et)_2$ detected below the limit of quantitation
[c] CHG(Et) not detected
[d] CHG(Et) detected, but not quantitated

in the liver. Therefore, this route of administration was not used in the efficacy studies described below.

Vehicle selection

HP-β-CD (20% in water) was selected as the vehicle of choice for the efficacy studies. Intravenous injection of dosing solutions containing HP-β-CD did not produce severe ulceration around the site of injection, unlike dosing solutions containing cremophor/ethanol. This allowed repeated delivery of $CHG(Et)_2$ by the i.v. route. The plasma pharmacokinetics of $CHG(Et)_2$ using HP-β-CD as a vehicle was similar to that obtained using cremophor/ethanol as a vehicle (data not shown). HP-β-CD formed a reversible complex with the *p*-chlorophenyl ring of $CHG(Et)_2$, indicated by the difference in the wavelength of maximum absorbancy of $CHG(Et)_2$ in

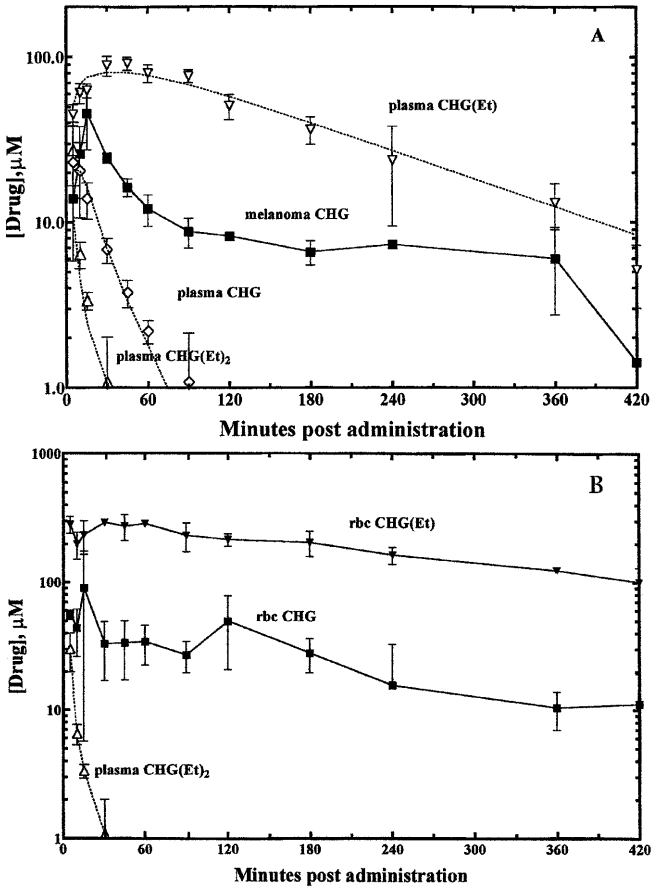

Fig. 3 **A** Plasma pharmacokinetics of $CHG(Et)_2$, CHG(Et) and CHG versus the pharmacokinetics of CHG in melanoma after a single bolus i.v. administration of $CHG(Et)_2$ to C57BL/6 (Es-1^e) female mice at 120 mg/kg. The dotted lines are the computer best-fit lines obtained from compartmental analysis of the plasma pharmacokinetics. **B** Red blood cell (*rbc*) pharmacokinetics of CHG and CHG(Et) versus the change in plasma concentration of $CHG(Et)_2$ after a single bolus i.v. administration of $CHG(Et)_2$ to C57BL/6 (Es-1^e) female mice at 120 mg/kg

buffered saline (pH 7.4, 25 °C; λ_{max} 259.5 nm, ε 13,000 $M^{-1}cm^{-1}$) versus that in 20% HP-β-CD in buffered saline (λ_{max} 264.0 nm, ε 14,024 $M^{-1}cm^{-1}$). The dissociation constant of the complex was 0.80 ± 0.03 mM obtained from the slope of a plot of the reciprocal of

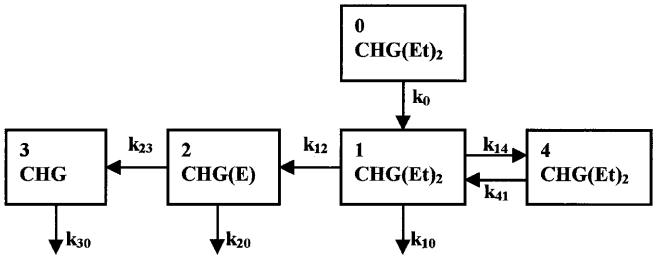

Fig. 4. Pharmacokinetic scheme

ΔOD_{264} of a buffered solution of $CHG(Et)_2$ versus the reciprocal of HP-β-CD concentration. The dissociation constant for the complex between HP-β-CD and $CHG(cyclopentyl)_2$ was similar in magnitude (K_{diss} 0.81 ± 0.04 mM).

Efficacy studies

In order to evaluate the chemotherapeutic potential of the glyoxalase I inhibitor, small-scale efficacy studies were carried out with C57BL/6 (Es-1^e) mice bearing murine B16 melanoma, and with athymic nude C57BL/6 (Es-1^e) mice bearing human prostate PC3 tumors or human colon HT-29 tumors.

B16 melanoma

Both $CHG(Et)_2$ and $CHG(cyclopentyl)_2$ were evaluated on the basis of the dosing schedule given in the legend to Fig. 5. Adriamycin was used as a positive control and was administered at 4 mg/kg on a schedule of four times daily for 3 days. The dicyclopentyl ester was selected for study because this compound is about twice as potent as the diethyl ester against tumors in culture [19]. Intravenous injection near the maximum tolerated doses of 120 mg/kg for $CHG(Et)_2$ and 139 mg/kg for $CHG(cyclopentyl)_2$ did not kill any of the mice, but produced a generalized negative physiological response in which the mice became immobilized (with twitching of the limbs) for several minutes. This was followed by

Table 4 Compartmental analysis of the plasma pharmacokinetic data for the sequential conversion of $CHG(Et)_2$ to CHG(Et) and CHG in C57BL/6 (Es-1^e) mice, after i.v. bolus administration of $CHG(Et)_2$ at 120 mg/kg. The kinetic data were fitted to the five-compartment open linear model shown in Fig. 4

Rate constant (min^{-1})	Female mice		Male mice	
	Tumor-bearing	Non-tumor-bearing	Tumor-bearing	Non-tumor-bearing
k_{12}	1.0×10^{-2}	1.7×10^{-2}	6.0×10^{-3}	1.1×10^{-2}
k_{10}	0.23	1.1	0.37	0.76
k_{23}	1.0×10^{-5}	5.4×10^{-4}	6.6×10^{-4}	1.4×10^{-3}
k_{20}	5.8×10^{-3}	5.6×10^{-3}	4.9×10^{-3}	1.3×10^{-2}
k_{30}	9.8×10^{-2}	3.6×10^{-2}	0.11	7.6×10^{-2}
k_{14}	6.0×10^{-2}	0.11	7.0×10^{-3}	16.5×10^{-2}
k_{41}	4.8×10^{-2}	8.6×10^{-2}	1.0×10^{-5}	7.7×10^{-2}
R^2 [$CHG(Et)_2$ data][a]	0.964	1.0	0.997	0.914
R^2 [CHG(Et) data][a]	0.939	0.742	0.820	0.946
R^2 [CHG data][a]	0.984	0.768	0.988	0.855

[a] Derived from a weighted least squares fit of the data

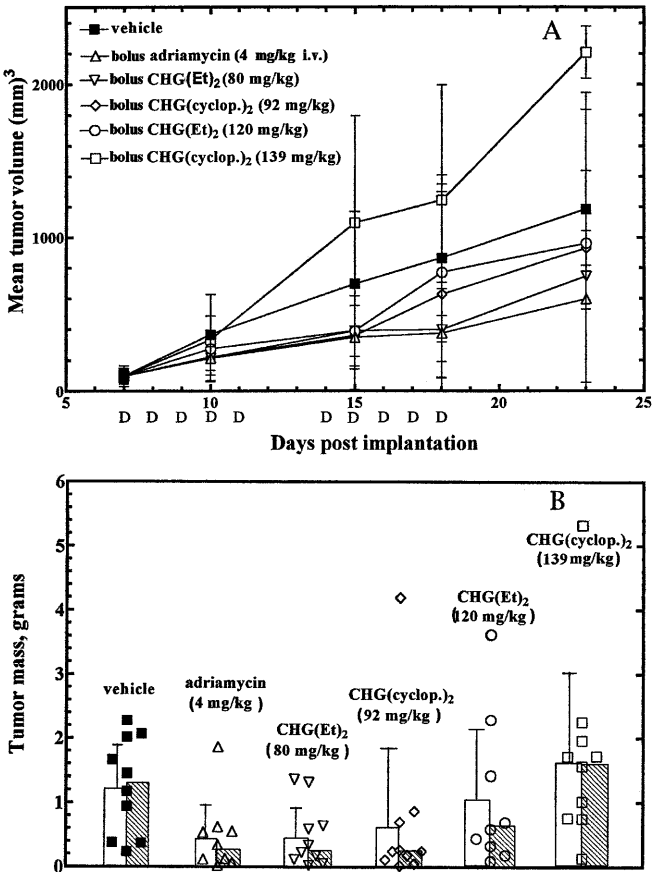

Fig. 5 **A** Mean tumor volumes of C57BL/6 (Es-1^e) mice bearing B16 melanotic melanoma treated by i.v. bolus administration of $CHG(Et)_2$ or $CHG(cyclopentyl)_2$ beginning on day 7 for 5 days a week for 2 weeks (*D* indicates day of treatment), or by i.p. bolus administration of Adriamycin on days 7, 11 and 15. **B** Post-necropsy tumor weights obtained on day 23 for all treatment groups (*symbols* indicate individual tumor weights; *open bars* and *lined bars* indicate mean and median values, respectively)

slow recovery to full activity over a period of about 15 min. These effects were not seen at the lower doses of 80 mg/kg for $CHG(Et)_2$ and 92 mg/kg for $CHG(cyclopentyl)_2$.

Mean tumor volumes are shown in Fig. 5A. No differences were noted between groups on day 7 or day 10. However, by day 15 tumor volumes of mice treated with $CHG(Et)_2$ at 80 mg/kg, $CHG(cyclopentyl)_2$ at 92 mg/kg, and Adriamycin were all significantly less than those of the vehicle control group on the basis of ANOVA ($P \leq 0.002$) and pair-wise comparisons using Dunnett's test. This trend continued through days 18 and 23. Day 23 was 5 days after the final treatment with $CHG(Et)_2$ and $CHG(cyclopentyl)_2$, and 8 days after the last treatment with Adriamycin. Median tumor volumes (not shown) followed the same trends. Post-necropsy tumor weights confirmed these drug effects (Fig. 5B). Dunnett's test indicated that the mean tumor weights of mice treated with the lower doses of $CHG(Et)_2$ and $CHG(cyclopentyl)_2$, and with Adriamycin were significantly less than those of the vehicle control group ($P \leq 0.05$). The Mann-Whitney test indicated that the median tumor weights of the low-dose and Adriamycin groups were significantly less than those of the vehicle control group ($P \leq 0.05$).

During the course of this study, no differences in either mean or median body weights were observed. Moreover, there were no significant differences in spleen, kidney or liver weights among the different treatment groups. Hematocrits obtained 5 days after treatment with either $CHG(Et)_2$ or $CHG(cyclopentyl)_2$ showed no differences between treatment groups by ANOVA or nonparametric analysis using the Kruskal-Wallis test.

PC3 prostate tumor

The melanoma study indicated that effective tumor growth inhibition could be achieved by reducing the maximum dose by 33%. Therefore, in the prostate cancer study, $CHG(Et)_2$ was evaluated at the lower dose of 80 mg/kg administered by i.v. bolus injection. For

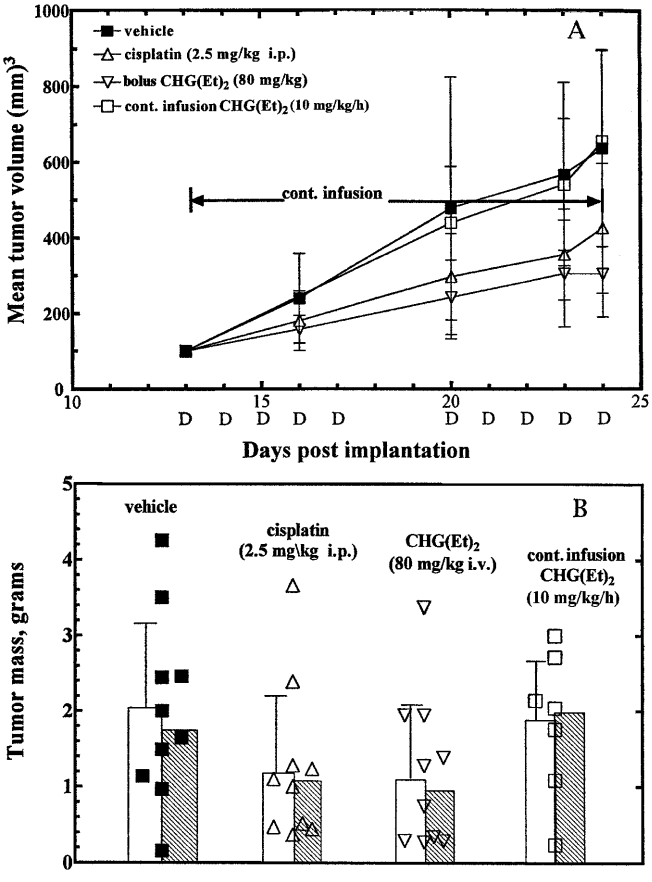

Fig. 6 **A** Mean tumor volumes of athymic nude (Es-1^e) mice bearing human prostate PC3 tumors treated by i.v. bolus administration of $CHG(Et)_2$ beginning on day 13 for 5 days a week for 2 weeks (*D* indicates day of treatment), or by i.p. bolus administration of cisplatin on days 13, 17 and 21. **B** Post-necropsy tumor weights obtained on day 24 for all treatment groups (*symbols* indicate individual tumor weights; *open bars* and *lined bars* indicate mean and median values, respectively)

comparison, $CHG(Et)_2$ administered as a continuous infusion by 14-day Alzet miniosmotic pumps was also evaluated. Cisplatin was used as a positive control and was administered near its maximum tolerated dose. There were no differences in mean tumor volumes between groups on day 16 (Fig. 6A). However, by day 20, tumor volumes of mice treated with $CHG(Et)_2$ at 80 mg/kg and with cisplatin at 2.5 mg/kg were all less than those of the vehicle control group on the basis of ANOVA ($P \leq 0.002$) and pair-wise comparisons using Dunnett's test. This trend continued through day 24. The mean and median post-necropsy tumor weights were significantly less for both of the above treatment groups in comparison with the vehicle control group ($P \leq 0.05$; Fig. 6A). There was no statistically significant difference in the tumor weights of the mice receiving $CHG(Et)_2$ by continuous infusion versus the vehicle controls.

During the course of this study, no differences in either mean or median body weights were observed. Spleen weights of mice treated with cisplatin were significantly less (about 36%) than those of the vehicle control group by nonparametric analysis using the Kruskal-Wallis test and the Mann-Whitney test ($P \leq 0.05$). There was no significant difference between the spleen weights of the mice treated with $CHG(Et)_2$ and those of the vehicle controls.

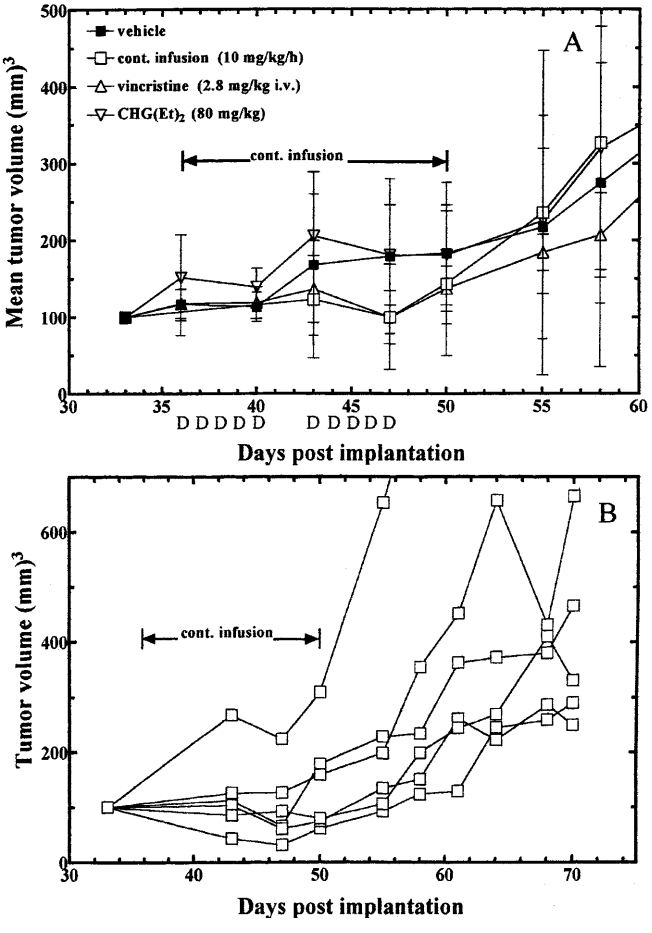

Fig. 7 **A** Mean tumor volumes of athymic nude Es-1^e mice bearing human colon HT-29 tumors treated with $CHG(Et)_2$ by either i.v. bolus administration for 5 days a week for 2 weeks or by continuous infusion beginning on day 36, or by i.v. bolus administration of vincristine on days 36, 40 and 44. **B** Tumor volumes for the individual mice in the group undergoing treatment by continuous infusion of $CHG(Et)_2$

HT-29 colon tumor

The effects of $CHG(Et)_2$ administered by i.v. bolus injection at 80 mg/kg or by continuous infusion were evaluated. Six mice were implanted with Alzet miniosmotic pumps for i.v. delivery of 1 *M* $CHG(Et)_2$ at a rate of 0.5 μl/h for 14 days. Treatment began on day 23 after tumor implantation. There were no differences in normalized tumor volumes between groups except on days 47 and 50 after tumor implantation (Fig. 7A). On these two days, immediately before and after treatment was terminated, the tumor volumes of the animals receiving vincristine on a schedule of four times daily for 3 days and of those receiving drug by continuous infusion were significantly less than the tumor volumes of the other groups. However, once treatment was stopped on day 49, the tumors grew rapidly, and there were no significant differences in tumor volumes at the end of the study. At termination, there were no significant differences in body, spleen and tumor weights among the different groups.

Discussion

While it is too early to predict the eventual role of glyoxalase inhibitors such as $CHG(Et)_2$ in cancer treatment, the work described here indicates that these compounds should be further explored as novel antitumor agents. The pharmacokinetic and efficacy studies showed that growth-inhibitory concentrations of CHG can be delivered into the tumors of tumor-bearing mice, depending upon the method by which the prodrug $CHG(Et)_2$ is administered. This is in general agreement with the findings of a previous study in which i.p. administration of the dicyclopentyl ester prodrug form of the glyoxalase I inhibitor *S-p*-bromobenzylglutathione at 200 mg/kg was found to inhibit the growth of murine adenocarcinoma 15A in mice by 40% [19]. The availability of a murine model with low plasma esterase activity allowed us to explore the feasibility of administering drug via the i.v. route. The specific activities of the glyoxalase enzymes in the organs of plasma esterase-deficient mice (Table 1) are similar to those previously reported for laboratory mice [8]. Therefore, the plasma esterase-deficient mice do not exhibit any apparent anomalies in terms of tissue glyoxalase activities. The V_m activities of both glyoxalase enzymes were significantly lower in melanoma tumor than in the normal tissues. This probably reflects lower levels of enzyme protein in

the tumor extracts and not the presence of endogenous inhibitors, as the apparent K_m values were similar to those reported for the purified mammalian enzymes [21]. The presence of competitive inhibitors would have increased the apparent K_m values. Low levels of glyoxalase II activity in tumors could be a marker for high sensitivity to the inhibitory effects of $CHG(Et)_2$, as previously discussed.

Pharmacokinetics

Intravenous administration of $CHG(Et)_2$ resulted in the rapid appearance of CHG in tissues, including melanoma. The in vitro binding assay indicated approximately 20% binding of $CHG(Et)_2$ to plasma protein. The loss of plasma prodrug ($T_{1/2}$ 8–16 min) was due primarily to rapid distribution into tissues as CHG(Et) and the powerful glyoxalase I inhibitor CHG (K_i 40 n*M*) (Tables 2 and 3). Presumably, this reflected rapid transport of $CHG(Et)_2$ into cells, followed by esterase-catalyzed hydrolysis to give CHG(Et) and CHG. Plasma CHG and CHG(Et) are unlikely to serve as significant sources of intracellular CHG and CHG(Et) given that the rates of diffusion of these species into L1210 cells in vitro are less than 5% of the rate observed with $CHG(Et)_2$ (Kavarana and Creighton, unpublished). We hypothesize that intracellular CHG inhibits tumor growth by inhibiting glyoxalase I and causing an increase in the intracellular concentration of methylglyoxal. The monoethyl ester CHG(Et) is also found in melanoma tumor and might contribute to growth inhibition, as this compound is a weak competitive inhibitor of human glyoxalase I (K_i 1.8 $\pm$ 0.5 μM). Red cell pharmacokinetics showed the accumulation of high concentrations of both CHG and CHG(Et) over 8 h. Also noteworthy was the detection of small but significant concentrations of CHG in brain tissue, indicating that $CHG(Et)_2$ diffuses across the blood-brain barrier.

Efficacy

The results of the efficacy studies with murine B16 melanotic melanoma and the two human tumor xenografts showed that under the right conditions $CHG(Et)_2$ can be used to deliver CHG into tumors at concentrations sufficient to inhibit tumor growth. The use of HP-β-CD as a vehicle proved to be critically important in these studies. This vehicle allowed multiple i.v. bolus injections without the localized necrosis observed near the site of injection when cremophore/ethanol was used.

For the murine melanoma study, i.v. bolus administration of $CHG(Et)_2$ at 67% of the maximum dose studied (80 mg/kg) proved to be as effective as Adriamycin administered at its maximum tolerated dose (Fig. 5). The alternative prodrug $CHG(cyclopentyl)_2$, when administered at the molar equivalent dose, was no more effective than $CHG(Et)_2$. The explanation for the diminished efficacy observed for both prodrugs when administered at the highest dose is not clear. Conceivably, high concentrations of drug might induce increased levels of the glyoxalase enzymes in tumor cells, thus overcoming the inhibitory effects of intracellular CHG. However, we could not find evidence for enzyme induction. The specific activities of the glyoxalase enzymes in melanoma tumors from vehicle control mice versus those in the treatment groups were identical within experimental error. Another possibility is that the negative physiological response induced in the mice at the highest dosing levels somehow retarded the distribution of drug into tumor tissue. This explanation is consistent with the results of a small-scale pharmacokinetic study in which the concentration of CHG in melanoma tumor after a single bolus i.v. administration of $CHG(Et)_2$ was not significantly different at a dose of 120 mg/kg than at 80 mg/kg, while plasma levels of prodrug displayed a linear response to dose.

In the efficacy studies with the human tumor xenografts, i.v. bolus administration of $CHG(Et)_2$ at 80 mg/kg inhibited PC-3 tumor growth as effectively as cisplatin administered near its maximally tolerated dose (Fig. 6). However, continuous infusion of $CHG(Et)_2$ had no significant effect on tumor growth. Apparently, this method of administration failed to deliver inhibitory concentrations of CHG to this rapidly growing tumor. Importantly, $CHG(Et)_2$ showed minimal side effects compared to cisplatin. Both nephrotoxicity and hemopoietic toxicity are notable side effects of treatment with this drug. Hemopoietic toxicity was indicated by the abnormally low spleen weights of the mice treated with cisplatin. There was no evidence for hemopoietic toxicity in mice receiving $CHG(Et)_2$; spleen weights were in the same range as those of the vehicle control mice. We suggest as a working hypothesis that the glyoxalase I inhibitor produces fewer side effects because (unlike cisplatin) this compound targets a peripheral metabolic difference between normal cells and cancer cells, rather than targeting the metabolic machinery within the nucleus of cells. In contrast, i.v. bolus administration of $CHG(Et)_2$ to mice bearing human colon HT-29 tumors did not inhibit tumor growth. However, continuous infusion of $CHG(Et)_2$ inhibited tumor growth about as well as vincristine administered as an i.v. bolus near its maximally tolerated dose (Fig. 7). These observations imply that the method of administering $CHG(Et)_2$ can be extremely important. Perhaps slow-growing tumors such as HT-29 are best treated by continuous infusion, while fast-growing tumors such as PC-3 tumors require bolus i.v. administration of drug in order to inhibit growth effectively.

In summary, we have developed quantitative HPLC methods for monitoring tissue levels of CHG and its hydrolysis products in biological matrices after either

i.v. or i.p. administration of the prodrug $CHG(Et)_2$ to plasma esterase-deficient mice. This allowed us to develop dosing protocols that deliver CHG to both murine tumors and human tumor xenografts in vivo at concentrations that inhibit tumor growth. Nevertheless, in order to inhibit tumor growth, high doses of drug must be delivered to the animals over long periods of time. Presumably, this is a reflection of the fact that CHG is both a reversible competitive inhibitor of glyoxalase I and is unstable inside tumor cells. A possible solution to this problem is to develop irreversible inhibitors of glyoxalase I that inactivate a significant fraction of glyoxalase I after brief exposure to the inhibitor.

References

1. Altman PL, Katz DD (1979) Inbred and genetically defined strains of laboratory animals: part 1, mouse and rat. Federation of American Societies for Experimental Biology
2. Ayoub FM, Allen RE, Thornalley PJ (1993) Inhibition of proliferation of human leukemia 60 cells by methylglyoxal in vitro. Leuk Res 17: 397
3. Ayoub F, Zaman M, Thornalley PJ, Masters J (1993) Glyoxalase activities in human tumor cell lines in vitro. Anticancer Res 13: 151
4. Baskaran S, Balasubramanian KA (1990) Toxicity of methylglyoxal towards rat enterocytes and colonocytes. Biochem Int 212: 166
5. D'Argenio DZ, Schumitzky A (1979) A package program for simulation and parameter estimation in pharmacokinetic systems. Comput Methods Programs Biomed 9: 115
6. Di Ilio C, Angelucci S, Pennelli A, Zezza A, Tenaglia R, Sacchetta P (1995) Glyoxalase activities in tumor and non-tumor human urogenital tissues. Cancer Lett 96: 189
7. Hamilton DS, Creighton DJ (1992) Inhibition of glyoxalase I by the enediol mimic S-(N-hydroxy-N-methylcarbamoyl)glutathione: the possible basis of a tumor-selective anticancer strategy. J Biol Chem 267: 24933
8. Jerzykowski T, Winter R, Matuszewski W, Piskorska D (1978) A reevaluation of studies on the distribution of glyoxalases in animal and tumor tissues. Int J Biochem 9: 853
9. Jimmerson VR, Shih T-M, Maxwell DM, Kaminskis A, Mailman RB (1989) The effect of 2-(o-cresyl)-4H-1:3:2-benzodioxaphosphorin-2-oxide on tissue cholinesterase and carboxylesterase activities of the rat. Fundam Appl Toxicol 13: 568
10. Kavarana MJ, Kovaleva EG, Creighton DJ, Wollman MB, Eiseman JL (1999) Mechanism based competitive inhibitors of glyoxalase I: membrane transport properties, in vitro antitumor activities, and stabilities in human serum and mouse serum. J Med Chem 42: 221
11. Lo TWC, Thornalley PJ (1992) Inhibition of proliferation of human leukaemia 60 cells by diethyl esters of glyoxalase inhibitors in vitro. Biochem Pharmacol 44: 2357
12. Murthy NSRK, Bakeris T, Kavarana MJ, Hamilton DS, Lan Y, Creighton DJ (1994) S-(N-Aryl-N-hydroxycarbamoyl)glutathione derivatives are tight-binding inhibitors of glyoxalase I and slow substrates for glyoxalase II. J Med Chem 37: 2161
13. Papoulis A, Al-Abed Y, Bucala R (1995) Identification of N^2-(1-carboxyethyl)guanine (CEG) as a guanine advanced glycation end product. Biochemistry 34: 648
14. Ray M, Halder J, Dutta SK, Ray S (1991) Inhibition of respiration of tumor cells by methylglyoxal and protection of inhibition by lactaldehyde. Int J Cancer 47: 603
15. Reiffen KA, Schneeder FA (1984) A comparative study on proliferation, macromolecular synthesis and energy metabolism of in vitro-grown Ehrlich ascites tumour cells in the presence of glucosone, galactosone and methylglyoxal. J Cancer Res Clin Oncol 107: 206
16. Richard JP (1991) Kinetic parameters for the elimination reaction catalyzed by triosephosphate isomerase and an estimation of the reaction's physiological significance. Biochemistry 30: 4581
17. Rocci ML, Jusko WJ (1983) LAGRAN program for area analysis and moments in pharmacokinetic analysis. Comput Programs Biomed 16: 203
18. Soares ER (1979) Identification of a new allele of Es-1 segregating in an inbred strain of mice. Biochem Genetics 17: 577
19. Thornalley PJ, Edwards LG, Kang Y, Wyatt C, Davies N, Ladan MJ, Double J (1996) Antitumor activity of S-p-bromobenzylglutathione cyclopentyl diester in vitro and in vivo. Biochem Pharmacol 51: 1365
20. Thornalley PJ, Ladan MJ, Ridgeway SJS, Kang Y (1996) Antitumor activity of S-(p-bromobenzyl)glutathione diesters in vitro: a structure activity study. J Med Chem 39: 3409
21. Vander Jagt DL (1989) The glyoxalase system. In: Dolphin D, Poulson R, Avramovic O (eds) Coenzymes and cofactors: glutathione, vol 3 (part A). John Wiley and Sons, p 152
22. Vince R, Daluge S (1971) A possible approach to anticancer agents. J Med Chem 14: 35
23. Vince R, Wolf M, Sanford C (1973) Glutaryl -S-(p-bromobenzyl)-L-cysteinylglycine. A metabolically stable inhibitor of glyoxalase I. J Med Chem 16: 951
24. White JS, Rees KR (1982) Inhibitory effects of methylglyoxal on DNA, RNA and protein synthesis in cultured guinea pig keratinocytes. Chem Biol Interact 38: 339